Neurodevelopmental mutation of giant ankyrin-G disrupts a core mechanism for axon initial segment assembly

Rui Yang[a,b], Kathryn K. Walder-Christensen[a,b], Samir Lalani[a,b], Haidun Yan[c], Irene Díez García-Prieto[d], Sara Álvarez[d], Alberto Fernández-Jaén[e], Laura Speltz[f], Yong-Hui Jiang[c,g,h], and Vann Bennett[a,b,1]

[a]Department of Biochemistry, Duke University, Durham, NC 27710; [b]Department of Cell Biology, Duke University, Durham, NC 27710; [c]Department of Microbiology and Molecular Genetics, Duke University, Durham, NC 27710; [d]Genomics and Medicine, NIM Genetics, 28049 Madrid, Spain; [e]Department of Pediatric Neurology, Hospital Universitario Quirón, 28223 Madrid, Spain; [f]Department of Neurology, University of Minnesota, Minneapolis, MN 55454; [g]Department of Neurobiology, Duke University, Durham, NC 27710; and [h]Department of Pediatrics, Duke University, Durham, NC 27710

Contributed by Vann Bennett, July 29, 2019 (sent for review June 11, 2019; reviewed by Christophe Leterrier and James L. Salzer)

Giant ankyrin-G (gAnkG) coordinates assembly of axon initial segments (AISs), which are sites of action potential generation located in proximal axons of most vertebrate neurons. Here, we identify a mechanism required for normal neural development in humans that ensures ordered recruitment of gAnkG and β4-spectrin to the AIS. We identified 3 human neurodevelopmental missense mutations located in the neurospecific domain of gAnkG that prevent recruitment of β4-spectrin, resulting in a lower density and more elongated pattern for gAnkG and its partners than in the mature AIS. We found that these mutations inhibit transition of gAnkG from a closed configuration with close apposition of N- and C-terminal domains to an extended state that is required for binding and recruitment of β4-spectrin, and normally occurs early in development of the AIS. We further found that the neurospecific domain is highly phosphorylated in mouse brain, and that phosphorylation at 2 sites (S1982 and S2619) is required for the conformational change and for recruitment of β4-spectrin. Together, these findings resolve a discrete intermediate stage in formation of the AIS that is regulated through phosphorylation of the neurospecific domain of gAnkG.

axon initial segment | giant ankyrin-G | β-4 spectrin | neurodevelopmental mutation | phosphorylation

Axon initial segments (AISs) are specialized plasma membrane compartments located in proximal axons of most vertebrate neurons and are sites of initiation of action potentials (1–4). The AISs of a subset of excitatory neurons also are targets of chandelier interneurons, which form axo-axonic GABAergic synapses that modulate neuronal excitability (5–7). AISs thus are cellular sites of signal integration where thousands of synaptic inputs result in a single output that can be tuned by GABA signaling.

Axon initial segments are capable of structural and compositional plasticity in response to neural activity, which may have a role in adaptive responses including some forms of learning and memory as well as during postnatal development of the nervous system (8–11). Signaling pathways directing assembly and plasticity of AISs have recently received attention. Protein kinase CK2 has been reported to promote binding of voltage-gated sodium channels (VGSCs) as well as KCNQ2/3 channels to ankyrin-G (12, 13), and may be regulated through cholinergic signaling (14). Regulation of myosin 2 activity through the phosphorylation state of its light chain has recently been identified as an important event in assembly and activity-induced plasticity of the AIS (15, 16). β4-spectrin has been identified as a binding partner for Ca^{2+}/calmodulin-dependent protein kinase II (CaMK2) at the AIS (17), although AIS substrates for CaMK2 are not known. Similarly, calcineurin (a calcium/calmodulin-regulated protein phosphatase) is required for positional plasticity of the AIS following chronic activation in cultured neurons (18), but the relevant protein substrates for calcineurin at the AISs are not known.

Assembly and function of the AIS critically depends on 480 kDa ankyrin-G (giant AnkG or gAnkG), which is a membrane-associated adaptor protein that coevolved with the AIS in early vertebrates (19). gAnkG-dependent binding partners localized at the AIS include voltage-gated sodium channels (20–23), KCNQ2/3 channels that modulate sodium channel activity (24, 25), 186 kDa neurofascin, a L1 CAM that directs GABAergic synapses to the AIS (20, 26), and β4-spectrin, which stabilizes the AIS (27, 28). Moreover, gAnkG is also required to form microtubule bundles at the AIS (22, 29, 30). gAnkG thus is a master organizer of the AIS (22, 23).

gAnkG contains the same canonical domains found in other ankyrins (ANK repeats, spectrin-binding domain, regulatory domain) plus a neurospecific domain encoded by a single giant exon inserted between the ZU5-UPA supermodule and death domain that is found only in vertebrates (19, 22, 31–33). The neurospecific domain has 2,606 residues that include a segment with modest sequence similarity to Titin, an elongated protein associated with sarcomeres. In addition, this domain also includes a 40-kDa

Significance

Axon initial segments of vertebrate neurons integrate thousands of dendritic inputs and generate a single outgoing action potential. Giant ankyrin-G associates with most of the molecular components of axon initial segments and is required for their assembly. This study identified 3 human mutations of giant ankyrin-G resulting in impaired neurodevelopment in compound heterozygotes. These mutations prevent transition of giant ankyrin-G from a closed to an open conformation, which normally is regulated by phosphorylation of giant ankyrin-G during maturation of axon initial segments. Giant ankyrin-G thus functions in a signaling pathway that may contribute to activity-dependent plasticity of the axon initial segment as well as provide a therapeutic target for treatment of patients bearing giant ankyrin-G mutations.

Author contributions: R.Y., K.K.W.-C., and V.B. designed research; R.Y., K.K.W.-C., S.L., H.Y., I.D.G.-P., and S.A. performed research; R.Y., K.K.W.-C., S.L., A.F.-J., L.S., Y.-H.J., and V.B. analyzed data; and R.Y. and V.B. wrote the paper.

Reviewers: C.L., Aix-Marseille University; and J.L.S., NYU School of Medicine.

The authors declare no conflict of interest.

See Commentary on page 19228.

[1]To whom correspondence may be addressed. Email: vann.bennett@duke.edu.

This article contains supporting information online at www.pnas.org/lookup/suppl/doi:10.1073/pnas.1909989116/-/DCSupplemental.

First published August 26, 2019.

serine- and threonine-rich subdomain that is modified by the O-GlcNac monosaccharide (34). The neurospecific domain interacts with multiple protein partners at the AIS, including GABARAP (35, 36), Nude1/NudeL1 (37), and microtubule end-binding (EB) proteins (23). Humans bearing a R1989W mutation of gAnkG that reduces the affinity for GABARAP by over a 1,000-fold have bipolar symptoms, while mice bearing the same mutation exhibit reduction in GABAergic synapses and hyperexcitability (38).

AnkG giant exons are conserved between humans and zebrafish, indicating strong evolutionary pressure to maintain amino acid sequence as well as preserve an uninterrupted exon (19, 22). Consistent with this high level of conservation, mice with targeted loss of gAnkG die around PND21 even though levels of 190 kDa AnkG are increased from 5- to 8-fold (22). Humans bearing a frame-shift mutation selectively targeting gAnkG survive in an institutional setting with intellectual impairment and other neurodevelopmental disorders (39).

In this study, we identify a role of the neurospecific domain of gAnkG in regulating recruitment of β4-spectrin during development of the axon initial segment. These experiments began with elucidation of the basis for reduced intensity of gAnkG assembly at the AIS due to 3 human neurodevelopmental missense mutations located in the gAnkG giant exon. We found that these mutations interfere with a major conformation change in gAnkG that is required for recruitment of β4-spectrin and result in arrested development of the AIS. We further found that the neurospecific domain is highly phosphorylated in mouse brain, and that phosphorylation at 2 sites (S1982 and S2619) is required for the conformational change and recruitment of β4-spectrin. Together, these findings suggest a potential mechanism for global regulation of structural and compositional plasticity at the AIS.

Results

Neurodevelopmental-Associated *ANK3* Mutations Target gAnkG. We identified 2 unrelated families, each with a child experiencing a neurodevelopmental disorder with compound heterozygosity for ANK3 mutations targeting the sequence encoded by exon 37, the neurospecific giant exon uniquely expressed in 480 kDa AnkG (gAnkG) (Fig. 1*A*). Both families also have a normal child with normal *ANK3* exome sequence. One child (male) carries compound heterozygous *ANK3* mutations at T1861M and P2490L, and was diagnosed with specific language disorder associated with mild autistic features when he was 5 y old (Fig. 1 *B*, *Left* and *SI Appendix*, Table S1). His mother, heterozygous for T1861M mutation, and his father, heterozygous for a P2490L mutation, are unaffected, while his unaffected sister has normal *ANK3* exome sequence (Fig. 1 *B*, *Left*). In the second family, a 7-y-old girl with compound heterozygous T1861M and K2864N *ANK3* mutations was diagnosed with multiple neurodevelopment disorders, including ataxia, developmental delay, cognitive impairment, and seizures (*SI Appendix*, Table S1). Her mother and father, who carry heterozygous mutation of T1861M or K2864N, respectively, are unaffected, while her unaffected sister has normal *ANK3* exome sequence (Fig. 1 *B*, *Right*). A video of the girl bearing T1861M/K2864N mutations can be found online (https://youtu.be/ZyHwlI5uERQ).

To evaluate functional consequence of gAnkG human mutations, we coexpressed mutant gAnkG-GFP with Cre-2A-BFP in hippocampal neurons from AG^{E22-23}fl/fl mice (loxP sites flanking exons 22 and 23 of *ANK3*) that lose all AnkG isoforms in the presence of Cre-recombinase (20). Neurons transfected with Cre-BFP 3 d following plating completely lost gAnkG labeling at the AIS at 7 d (*SI Appendix*, Fig. S1). We cotransfected AG^{E22-23}fl/fl neurons with plasmids encoding Cre-BFP and gAnkG-GFP that was either wild type (WT) or bearing 1 of the 3 human mutations (T1861M, K2864N, and P2490L). gAnkG-GFP bearing human mutations targeted to the proximal axon. However, all 3 mutant versions of gAnkG-GFP exhibited a less intense and more extended labeling pattern than either WT gAnkG-GFP or endogenous gAnkG (Fig. 1*C*). To quantitatively display the distribution of gAnkG at AIS, we linearly aligned the gAnkG pixel intensity from the beginning to the end of enrichment at the axon as described by Berger et al. (16). gAnkG-GFP bearing either T1861M, K2864N, or P2490L mutations showed an extended pattern, combined

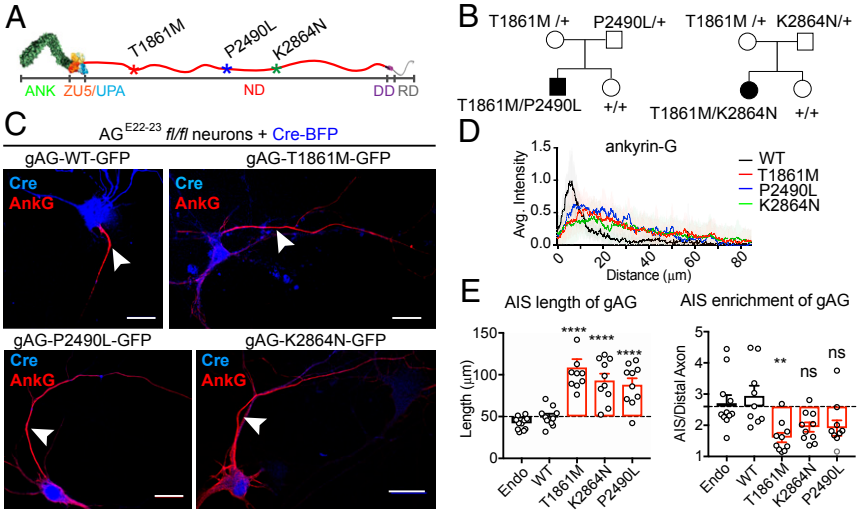

Fig. 1. Newly identified human neurodevelopment disorder mutations of *ANK3* impair gAnkG targeting to the AIS. (*A*) Schematic of the gAnkG polypeptide. Ankyrin repeats (ANK), ZU5/UPA domain, neurospecific domain (ND), death domain (DD), and regulatory domain (RD) are indicated. Asterisks indicate amino acid positions of human mutations. (*B*) Pedigrees of affected individuals with corresponding compound heterozygous mutations. (*C*) The 3 DIV hippocampal neurons from AG^{E22-23}fl/fl mice were cultured and cotransfected with Cre-2A-BFP and plasmids encoding gAnkG-EGFP that were either WT or bearing human mutations. Transfected neurons were fixed at 7 DIV and stained with an AnkG antibody. Representative images are shown for Cre (blue) and AnkG staining (red) (Scale bar, 20 μm.) (*D*) Average intensity of AnkG staining at the AIS is plotted and aligned for neurons transfected with WT gAnkG (black) or gAnkG with human mutations (red for T1861M, blue for P2490L, and green for K2864N). $n = 10$ and results are repeated in 3 independent neuronal cultures. (*E*) Quantification of the length and the enrichment of AnkG at the AIS of transfected neurons. Mean ± SEM; $^{**}P = 0.005$, $^{****}P < 0.0001$; 1-way ANOVA followed by Dunnett's multiple comparisons test; $n = 10$; experiments were repeated in 3 independent cultures; ns, not significantly different.

with lower peak intensity compared to wild-type gAnkG-GFP (Fig. 1*D*). We measured the length of axonal accumulation of gAnkG-GFP beginning in the proximal axon continuing along the axon to the point where the intensity dropped to the background level, defined as the intensity of the distal axon 100 μm from the cell body. gAnkG-GFP-bearing human mutations exhibited staining intensity above background for ∼70 to 100 μm, which is nearly 2 times longer than transfected wild-type gAnkG-GFP or endogenous AnkG, where staining intensity fell to background levels within 50 μm (Fig. 1 *D* and *E*). We also measured the enrichment of gAnkG by dividing its peak intensity at the AIS by the distal axon intensity measured 100 μm from the cell body. gAnkG-GFP bearing human mutations showed a reduced maximal enrichment of ∼1.5- to 2-fold compared to an average enrichment of ∼3-fold for wild-type gAnkG-GFP or endogenous gAnkG (Fig. 1*E*).

Neurodevelopmental ANK3 Mutations Repress gAnkG Recruitment of β4-Spectrin. We next investigated how human mutations of gAnkG affect AIS recruitment of its molecular partners β4-spectrin, 186 kDa neurofascin, and VGSCs. Targeting of all 3 proteins to the AIS is completely abolished in AG^{E22-23}fl/fl neurons transfected with Cre-BFP (*SI Appendix*, Fig. S1) and is fully restored by transfection of wild-type gAnkG-GFP (Fig. 2 *A*, *Left* column). However, neurons transfected with gAnkG-GFP bearing neurodevelopmental mutations exhibit markedly reduced recruitment of β4-spectrin (Fig. 2*A*). In contrast, 186 kDa neurofascin and VGSCs, both copatterned with mutant gAnkG-GFP, and exhibited the same extended and less intense pattern compared to neurons expressing WT gAnkG-GFP (Fig. 2*A*). Densitometry revealed that the peak intensity of neurofascin and VGSCs of transfected neurons dropped to about half compared to WT neurons. Also, the width of the curve was increased in transfected neurons (Fig. 2*B*). In contrast, staining for β4-spectrin at the AIS was almost completely lost (Fig. 2 *B*, *Top*). Taken together, *ANK3* neurodevelopmental mutations selectively impair gAnkG recruitment of β4-spectrin to the AIS, while 186 kDa neurofascin and VGSCs copattern with gAnkG.

β4-Spectrin Is Required for Assembly of a Compact AIS. Two major alternatively spliced variants of β4-spectrin, termed Σ1 and Σ6, are located at the AIS (*SI Appendix*, Fig. S2*A*) (27, 40). β4-spectrin-Σ6 lacks the N-terminal actin- and adducin-binding domains and spectrin repeats 1 through 9, but shares the C-terminal region, including the AnkG-binding site, located in spectrin-repeat 15, and a PH domain; Fig. 3*A*). To understand how impaired recruitment of β4-spectrin altered AIS morphology, we knocked out both Σ1 and Σ6 isoforms in neurons by CRISPR-Cas9 using gRNA targeting a shared exon (Fig. 3*A*). We confirmed elimination of β4-spectrin expression in β4-spectrin gRNA transfected neurons by immunostaining neurons using a β4-spectrin antibody recognizing both Σ1 and Σ6 isoforms (Fig. 3 *A*–*C*). Then, we determined the distribution pattern of AnkG and its binding partners. In CRISPR-Cas9 transfected neurons, gAnkG, neurofascin, and VGSCs accumulated in a longer and less concentrated pattern at the AIS, when compared to nontransfected neurons on the same coverslip (Fig. 3 *B* and *C*). β4-spectrin knockout thus phenocopies the effect of gAnkG human mutations (Fig. 2).

Transfection of pan-β4-spectrin knockout neurons with β4-spectrin-Σ1-Halo restored a compact AIS pattern for gAnkG, as well as for 186 kDa neurofascin, and VGSC (*SI Appendix*, Fig. S2*B*). Interestingly, the shorter Σ6 isoform of β4-spectrin-Halo lacking the N-terminal actin/adducin binding domains also rescued the phenotype (Fig. 3 *E* and *F*). This finding suggests the actin- and adducin-binding domains of β4-spectrin are not required for the assembly of the AIS in cultured neurons, while the C-terminal half, which includes the AnkG-binding site and PH domain as well as a CAMK2-binding site (17), is essential.

β1- and β2-spectrins bind to ankyrin ZU5 domains in a canonical interaction involving a critical tyrosine (Y1874 in human beta-2 spectrin) located in spectrin-repeat 15 that is conserved in

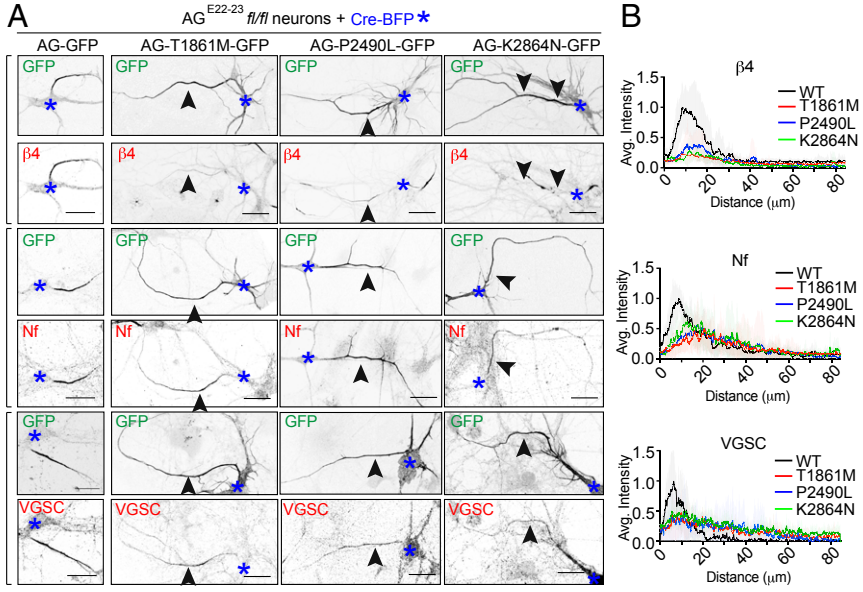

Fig. 2. Human mutations of gAnkG repress β4-spectrin recruitment to the AIS. (*A*) The 3 DIV hippocampal neurons cultured from AG^{E22-23}fl/fl mice were transfected with plasmids encoding Cre-BFP and either wild-type gAnkG-GFP or gAnkG-GFP bearing human mutations T1861M, K2864N, and P2490L. Transfected neurons were fixed and stained with antibody against AnkG (AG), β4-spectrin (β4), 186 kDa neurofascin (Nf), or VSVGs. Confocal fluorescent images of transfected neurons are displayed for GFP signal of gAnkG and indicated antibody staining. Blue asterisks indicate the cell body of transfected neurons and black arrowheads point to the AIS from the same neuron (Scale bar, 20 μm.) (*B*) Average intensity of indicated antibody staining at the AIS is plotted for neurons transfected with wild-type gAnkG (black) or gAnkG with individual human mutation (red for T1861M, blue for P2490L, and green for K2864N). $n = 10$ and results were repeated in 3 independent neuronal cultures.

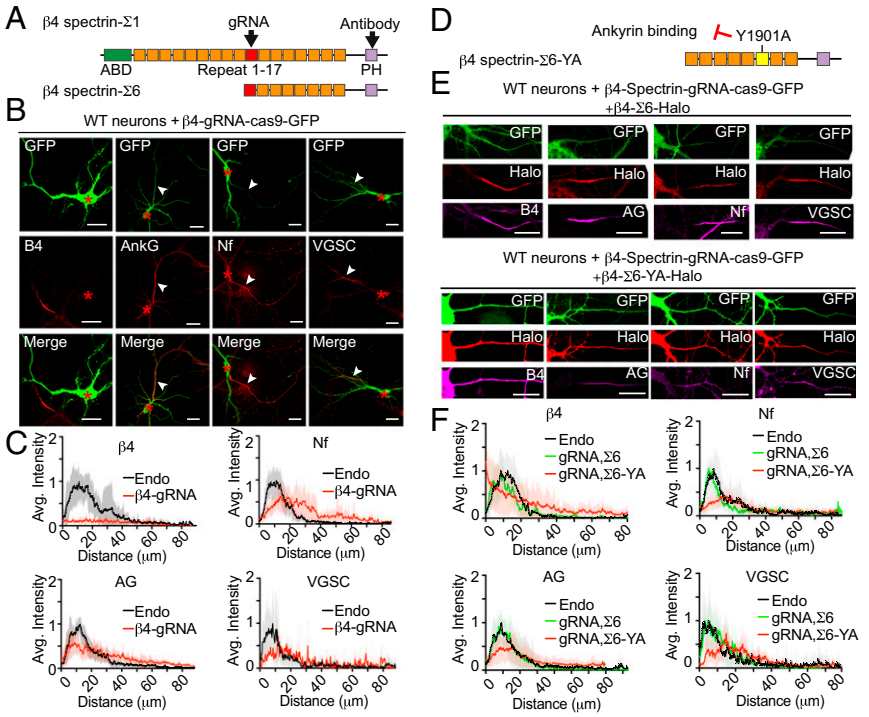

Fig. 3. Knockout of β4-spectrin phenocopies human neurodevelopmental *ANK3* mutations. (*A*) Schematic of β4-spectrin-Σ1 and Σ6 polypeptides. Actin-binding domain (ABD), pleckstrin homology domain (PH), and the 17 spectrin repeats (SRs) are indicated. The target sites of gRNA and the spectrin antibody are indicated with black arrowheads. (*B*) Wild-type hippocampal neurons were transfected on 3 DIV with a single construct containing CRISPR-Cas9 cDNA fused with GFP and a gRNA targeting β4-spectrin. Neurons were fixed at 7 DIV and stained with indicated antibodies. Red asterisks indicate the cell body of transfected neurons and white arrowheads indicate the position of AISs (Scale bar, 20 μm.) (*C*) Average intensity of indicated antibody staining at the AIS is plotted and aligned for β4-spectrin gRNA transfected neurons (red line) and nontransfected neurons (endo, black line) on the same coverslip. $n = 10$. Results were repeated in 3 independent cultures using gRNA targeting 4 different regions. (*D*) Schematic of β4-spectrin-Σ6 labeled with Y1901A mutation site, which eliminated the interaction with ankyrin. The AnkG-binding region in SR 15 is highlighted in yellow. (*E*) The 3 DIV wild-type hippocampal neurons were cotransfected with β4-spectrin-gRNA and β4-spectrin-Σ6-Halo or Σ6-YA-Halo. On 7 DIV, neurons were incubated with JF549 halo dye followed by staining with indicated antibody (Scale bar, 20 μm.) (*F*) Average intensity of indicated antibody along the AIS is plotted for transfected neurons (β4-spectrin-Σ6 rescue in green line and YA mutant rescue in red line) and aligned with nontransfected neurons (endo, black line). $n = 10$ of each plot. Results were repeated in 3 independent experiments.

β4-spectrins (41–43). We determined the effect of Y1901A mutation of sigma 6 β4-spectrin (corresponding to Y1874A mutation of beta-2 spectrin) on β4-spectrin activity in rescuing pan-β4-spectrin knockout neurons (Fig. 3*D*). Sigma 6 β4-spectrin bearing a Y1901A mutation did not target to the AIS, and instead evenly distributed over the entire cell (Fig. 3*E*). The intensity of β4-spectrin labeling along the AIS actually progressively decreased in the proximal axon compared to the cell body (Fig. 3*F*). Y1901A β4-spectrin, in contrast to wild-type β4-spectrin, did not restore labeling of gAnkG, neurofascin or VGSCs, and thus failed to rescue the morphology of AIS (Fig. 3 *E* and *F*). β4-spectrin therefore requires a canonical interaction with gAnkG for its assembly and function at the AIS.

Phosphorylation of Ser1982 and Ser2619 of gAnkG Drives AIS Recruitment of β4-Spectrin. To summarize so far, our data reveal that loss of β4-spectrin phenocopies consequences of 3 different gAnkG neurodevelopmental mutations targeting its neurospecific domain (T1861M, P2490L, and K2864N). We also find that AIS targeting and function of β4-spectrin requires its canonical interaction with gAnkG through the first ZU5 domain (residues 982 through 1,086), which is distant from sites of neurodevelopmental mutations (T1861–K2864). These findings raise the question of how neurodevelopmental mutations of gAnkG abolish β4-spectrin recruitment. It is pertinent in this regard that S2417A mutation of gAnkG in giant exon 37 also eliminates its ability to recruit β4-spectrin to the AIS, while the S2417D phosphomimetic mutant retains activity, suggesting that gAnkG recruitment of β4-spectrin may be regulated by phosphorylation (22). These considerations suggest the hypothesis that neurodevelopmental mutations of gAnkG either directly or indirectly interfere with a physiological pathway that regulates gAnkG recruitment of β4-spectrin through phosphorylation of gAnkG in its neurospecific domain. As a first test of this hypothesis, we determined the phosphorylation state of gAnkG in brain tissue.

We performed LC-MS/MS to evaluate posttranslational modification of AnkG polypeptides immunoisolated from day 60 mouse brain without using titanium dioxide to concentrate phosphorylated peptides (Fig. 4). By not having an enrichment step, we were able to estimate stoichiometries of the phosphospecies as both phosphopeptides and corresponding nonphosphorylated peptides are captured by the mass spectrometer. We found phosphorylation of serine 2417 (2406 in the human cDNA) with an abundance of 8%, as well as multiple serine and threonine sites with higher abundance, all located within the neurospecific domain (Fig. 4*A*) (22).

To address the physiological function of these phosphorylation sites, we determined effects of S/A or T/A mutation on ability of gAnkG-GFP to restore AIS recruitment of gAnkG and its partners in AnkG-null neurons. We mutated 9 high stoichiometry phosphorylation sites (percent abundance greater than 10%) and verified that these gAnkG mutants were expressed as full-length polypeptides in HEK293 cells (Fig. 4*A* and *SI Appendix*, Fig. S3).

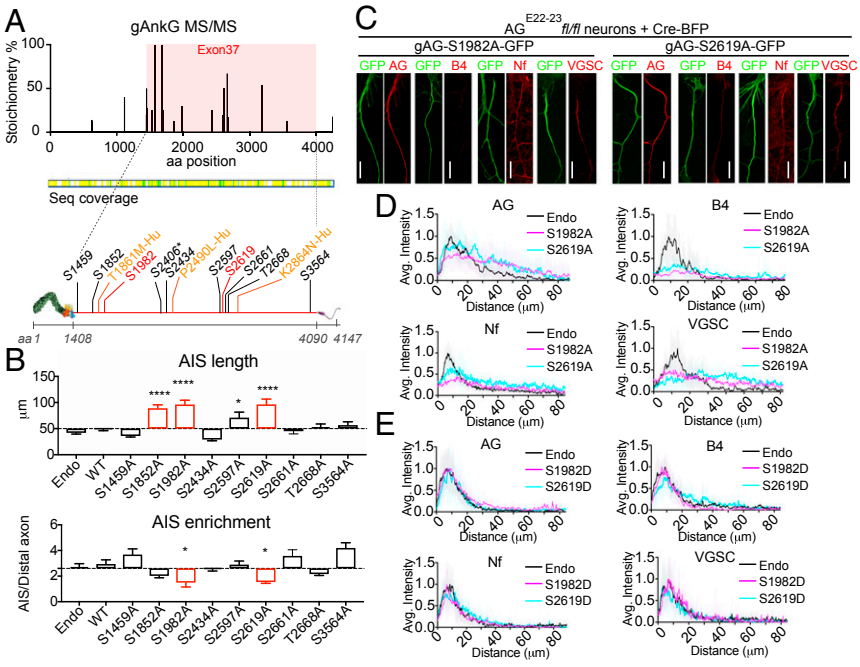

Fig. 4. Phosphorylation of gAnkG at S1982 and S2619 is required for recruitment of β4-spectrin to the AIS. (*A*) MS-MS detected multiple high stoichiometry phosphorylation sites (>10%) in exon 37-encoded sequence from AnkG isolated from mouse brain by immunoprecipitation (*SI Appendix, SI Materials and Methods*). Locations of screened phosphorylation sites (black and red) and human neurodevelopmental disorder mutations (yellow) in gAnkG. Asterisk-labeled site S2406 corresponds to S2417 in mouse sequence. (*B*) Hippocampal neurons from AG^{E22-23}fl/fl mice were cotransfected on day 3 with plasmids encoding Cre-BFP and gAnkG-GFP bearing serine/threonine to alanine mutants at indicated amino acid sites. Neurons were fixed and stained with AnkG antibody at 7 DIV. The length and the enrichment of AnkG at AIS is quantified. Mean ± SEM; *$P < 0.05$; ****$P = 0.0001$; 1-way ANOVA followed by Dunnett's multiple comparisons test; $n = 10$ from 3 independent experiments. (*C*) AG^{E22-23}fl/fl neurons transfected with plasmids encoding Cre-BFP and non-phosphorylatable gAnkG mutants (gAG-S1982A-GFP or gAG-S2619A-GFP) were stained with indicated antibody. (Scale bar, 20 μm.) (*D*) Average intensity of indicated antibody at the AIS is plotted (S1982A in magenta; S2619A in blue) and aligned with nontransfected neurons (endo, black line). $n = 10$ of each plot. Results were repeated in 3 independent experiments. (*E*) Average intensity of indicated antibody at the AIS is plotted for AG^{E22-23}fl/fl neurons cotransfected with plasmids encoding Cre-BFP and phosphomimetic gAnkG mutants (S1982D in magenta or S2619D in blue) and aligned with nontransfected neurons (endo, black line). $n = 10$ of each plot. Results are repeated in 3 independent experiments.

Alanine mutation of residues S1852 (12% abundance), S1982 (30% abundance), or S2619 (50% abundance) significantly increased the length of AnkG accumulation at AISs (Fig. 4 *B*, *Top*; $P < 0.0001$, $n = 10$). Furthermore, S1982A and S2619A mutants showed a decreased enrichment of AnkG at the AIS, which phenocopied the AnkG neurodevelopmental mutations (Fig. 4 *B*, *Bottom*, $P < 0.01$, $n = 10$; Fig. 2). We then evaluated how S1982A and S2619A affect the recruitment of other AnkG AIS binding patterners. S1982A and S2619A mutation of gAnkG nearly eliminated the recruitment of endogenous β4-spectrin to the AIS. In addition, these mutations resulted in elongated and less concentrated patterns of neurofascin and VGSCs at the AIS (Fig. 4 *C* and *D*). In contrast, S1982D and S2619D phosphomimetic mutants of gAnkG functioned equivalently to WT gAnkG in assembly of the AIS (Fig. 4*E*).

In summary, we present direct evidence that gAnkG is phosphorylated in mouse brain and identify 2 phosphorylation sites (S1982 and S2619) that are critical for function of gAnkG in recruiting β4-spectrin to the AIS. We further demonstrate that alanine mutation preventing gAnkG phosphorylation at either site phenocopies neurodevelopmental gAnkG mutations, while the corresponding phosphomimetic mutations to aspartic acid exhibit full activity.

gAnkG Exon 37 Mutations Impair Interaction of gAnkG and β4-Spectrin. β4-spectrin requires interaction with gAnkG in order to target to the AIS in vivo and in cultured neurons (20, 22, 27). To determine how neurodevelopmental and phosphorylation site mutations affect gAnkG interaction with β4-spectrin, we initially attempted to express and purify these proteins in HEK293 cells in order to measure their interactions in biochemical assays. However, we were not successful in isolating gAnkG, due in part to its unusual sensitivity to protease digestion. We therefore modified a previously reported cellular assay where coexpression of AnkG-GFP with neurofascin in HEK293T cells results in recruitment of AnkG-GFP from the cytoplasm to the plasma membrane (*SI Appendix*, Fig. S4*A*) (44). We selected T1861M and S1982A mutations as representative of neurodevelopmental and phosphorylation site mutations, respectively. We first established that HA-186 kDa neurofascin recruited WT as well as T1861M and S1982A mutant gAnkG-GFP to the plasma membrane (*SI Appendix*, Fig. S4*B*). We next determined that Halo-tagged sigma 6 beta 4-spectrin relocated to the plasma membrane in HEK293 cells only when coexpressed with both HA-186 kDa neurofascin and gAnkG-GFP (*SI Appendix*, Fig. S4*C* and Fig. 5 *B* and *C*). Halo-tagged β4-spectrin bearing a Y1901A mutation was not recruited to the plasma membrane by gAnkG (Fig. 5 *B* and *C*), indicating that β4-spectrin interacts with gAnkG through its ZU5 domain. Interestingly, gAnkG-DAR999AAA mutation in the ZU5 domain did not prevent membrane recruitment of β4-spectrin, even though this mutation abolishes binding to β2-spectrin (Fig. 5 *B* and *C*) (43). These results indicate that the ZU5 domain of gAnkG interacts differently with spectrin-repeat 15 residues of β2-spectrin and β4-spectrin. We next determined whether the neurodevelopmental T1861M and/or S1982A mutations disrupted interaction between gAnkG and β4-spectrin. We found that targeting of β4-spectrin to the plasma membrane was markedly reduced by both gAnkG T1861M and S1982A mutations (Fig. 5 *B* and *C*). This

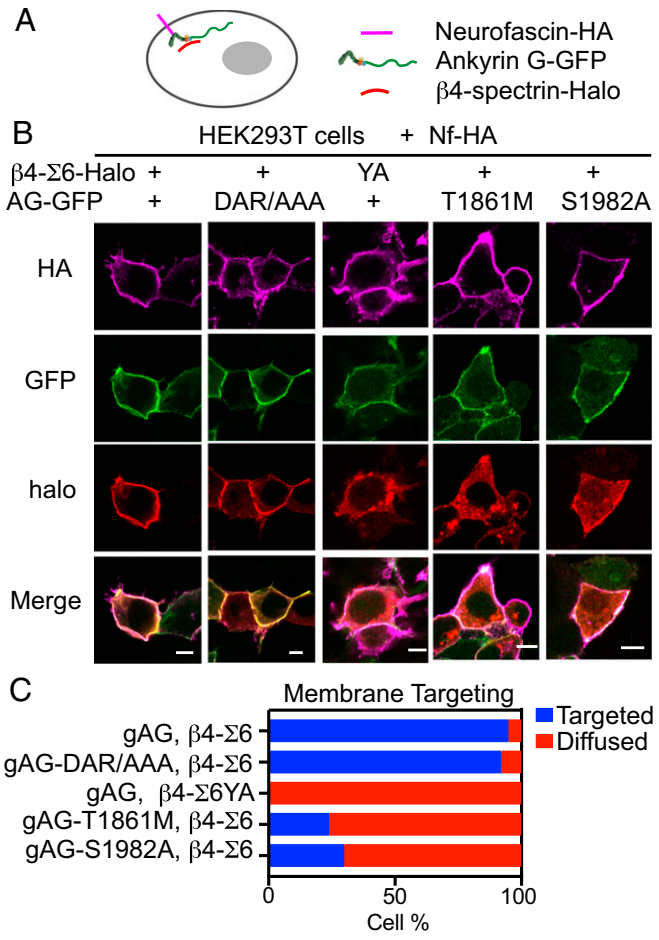

Fig. 5. β4-spectrin and AnkG interaction is impaired by the gAnkG human T1861M mutation and the nonphosphorylatable S1982A mutation. (*A*) Schematic demonstrating 186 kDa neurofascin recruitment of gAnkG and spectrin to the cell membrane. (*B*) Images of HEK293T cells transfected with plasmids encoding neurofascin-HA, β4-spectrin-Halo and gAnkG-GFP or β4-spectrin-halo and gAnkG-GFP bearing indicated mutations. Cells were labeled with JF594 halo dye and stained with antibody against neurofascin (Scale bar, 10 μm.) (*C*) The number of transfected HEK293T cells that show a clear membrane targeting of β4-spectrin is quantified ($n > 20$ cells from 3 independent experiments).

result was unexpected because, as noted above, the canonical spectrin-binding site of gAnkG is located in the first ZU5 domain (residues 982 through 1,086) and is distant from mutation sites (42).

Altogether, our data suggest that interaction between gAnkG and beta 4-spectrin depends on the Y1901 in spectrin-repeat 15, and thus involves the gAnkG ZU5 domain. However, T1861M neurodevelopmental mutation and S1982A loss of phosphorylation mutations within the neurospecific domain of gAnkG inhibit recruitment of β4-spectrin to the plasma membrane, which likely involves an indirect mechanism that will be addressed below.

Giant AnkG Is Locally Activated by a Conformation Change at the AIS. We next sought to understand how multiple mutation sites spread across ∼1,000 amino acids and distant from the direct spectrin-binding site in gAnkG could impair gAnkG recruitment of β4-spectrin. gAnkG at the AIS is ∼150 nm in length based on imaging by immunogold platinum replica electron microscopy and presumably lacks contact between C-terminal and N-terminal domains (22). However, structural studies indicate that the unstructured C-terminal regulatory domain of AnkG can interact with the peptide-binding groove of N-terminal ANK repeats, potentially resulting in autoinhibition (45). We hypothesized that interactions between C-terminal and N-terminal domains do occur in mutant gAnkG polypeptides and contribute to loss of β4-spectrin binding activity. To test this idea, we performed a proximity ligation assay (PLA) in neurons using a mouse anti-AnkG-N-terminal antibody generated against a synthetic peptide derived from the AnkG spectrin-binding domain (Life Technologies 33-8800) and a rabbit anti-AnkG-C-terminal antibody generated against the AnkG C-terminal domain expressed in bacteria (46), which would be expected to yield a positive signal only when the distance between N- and C-terminal domains is less than 40 nm (Fig. 6*A*). The specificities of N- and C-terminal AnkG antibodies were validated using 2 chimeric AnkB/AnkG polypeptides (47). The Ank-BBG polypeptide, containing ankyrin repeats, ZU5, and UPA domains of AnkB and C-terminal domain of AnkG specifically interacted with C-terminal AnkG antibody, whereas Ank-GGB, containing the ankyrin repeats, ZU5, and UPA domains of AnkG and C-terminal domain of AnkB, specifically interacted with N-terminal AnkG antibody (*SI Appendix*, Fig. S5 *A* and *B*).

N- and C-terminal AnkG antibodies both showed clear staining of the AIS (Fig. 6*A*). However, even though considerable PLA signal was evident at the cell body and dendrites, very low PLA signal was detected at AIS in the same cells using these antibodies (Fig. 6 *A* and *B*). The lack of PLA signal at the AIS is consistent with gAnkG in an extended conformation, where the N- and C- terminal domains are separated by at least 40 nm. PLA signal at the cell body could result from contributions by either 190 kDa AnkG, where N- and C-terminal domains are not separated by the neurospecific domain, and/or by gAnkG in an inactive conformation. To resolve these possibilities, we compared PLA signals from $AnkG^{E22-23}$fl/fl neurons transfected with Cre-BFP and either 190 kDa AnkG-GFP or gAnkG-GFP. One hundred ninety kDa AnkG-GFP was distributed throughout the neuron, including both dendritic and axonal compartments, and produced PLA signals evenly distributed across the cell (Fig. 6 *C*, *Left*). Strikingly, even though gAnkG-GFP is highly enriched at the AIS, the PLA signal was much lower at the AIS than in somatodendritic areas (Fig. 6 *C*, *Right*). Comparison of PLA signals in 190 kDa or gAnkG-GFP expressing neurons showed no difference in dendrites (Fig. 6*D*, $P > 0.05$, $n = 10$) but a major reduction in the PLA signal for gAnkG at the AIS (Fig. 6*D*, $P < 0.0001$, $n = 10$). This suggests that the majority of gAnkG-GFP at the AIS exists an extended conformation with separated N- and C-termini, while gAnkG-GFP outside of the AIS is configured with closely opposed N- and C-termini.

We next determined PLA signals at the AIS generated by mutant gAnkG-GFP polypeptides with impaired β4-spectrin recruitment activity. We transfected AG^{E22-23}fl/fl neurons with Cre-BFP and gAnkG-GFP bearing either neurodevelopmental mutations (T1861M, P2490L, and K2864N) or nonphosphorylatable mutations (S1982A and S2619A). Strikingly, these mutated gAnkG polypeptides all exhibited a gain of PLA signal at the AIS, even though mutated gAnkG-GFP was present in lower concentration than WT gAnkG-GFP (Fig. 6 *E* and *F*). Thus, multiple gAnkG mutations that impair β4- spectrin recruitment also promote close proximity between N- and C-terminal domains. We sought to confirm the change of gAnkG conformation using fluorescence resonance energy transfer (FRET) by adding a donor tag (mClover) and a receiving tag (mScarlet-I) on N- and C-ends of gAnkG, respectively. However, modification of the N-terminus by addition of a fusion tag prevented targeting of gAnkG to the AIS in multiple experiments.

Loss of gAnkG N-/C-Terminal Domain Interaction Parallels AIS Assembly. The length and position of the AIS within axons is regulated during neuronal development and in homeostatic responses to excitation (9, 11, 48). To test whether the gAnkG

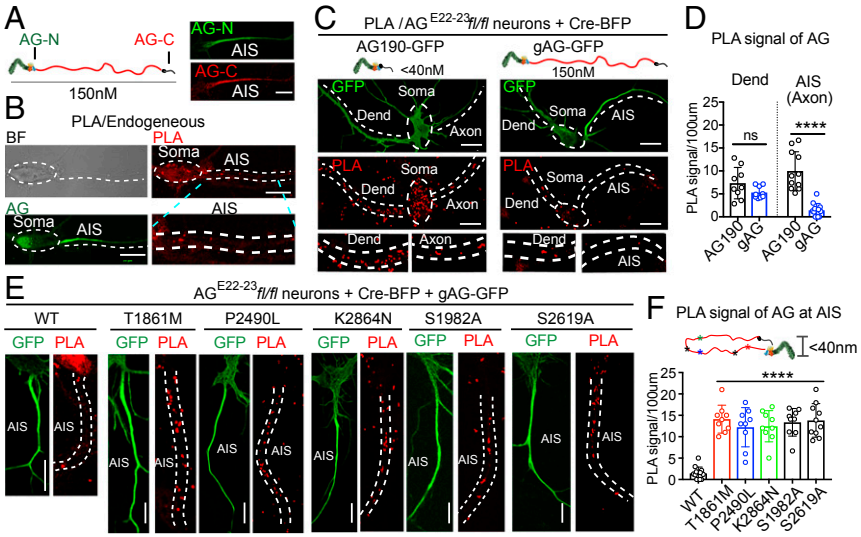

Fig. 6. Proximity ligation assay of N- and C-ends of gAnkG reveals an extended conformation at the AIS that is lost in mutant gAnkG. (*A*, *Left*) Recognition sites of antibody against the N-terminal (AG-N) or C-terminal (AG-C) of gAnkG used in PLA. (*A*, *Right*) Immunostaining of the AIS by AG-N and AG-C in 7 DIV hippocampal neurons (Scale bar, 10 μm.) (*B*) PLA in 7 DIV hippocampal neurons. Bright filled, AnkG and PLA images are displayed from top to bottom. The soma and AIS region of the neurons is labeled with white dash lines. The PLA signal of AIS is enlarged (Scale bar, 10 μm.) (*C*) PLA of 7 DIV AG^{E22-23}fl/fl neurons cotransfected with plasmids encoding Cre-BFP and either 190 kDa-AnkG-GFP (*Left*) or gAnkG-GFP (*Right*). Representative images of GFP and PLA signal of transfected neurons are shown. PLA signals in dendrites and proximal axon are enlarged (Scale bar, 10 μm.) (*D*) PLA signals at the AIS and dendrite are quantified. Mean ± SEM, $^{****}P = 0.0001$, *t* test, $n = 10$ from 3 independent experiments; ns, not significantly different. (*E*) PLA of 7 DIV cultured hippocampal AG^{E22-23}fl/fl neurons cotransfected with Cre-BFP and wild type or indicated gAnkG-GFP mutants. Representative images of GFP and PLA signal of transfected neuron AISs are shown (Scale bar, 10 μm.) (*F*) Schematic showing a potential conformation change in gAnkG mutations. PLA signals at the AIS are quantified. Mean ± SEM, $^{****}P = 0.0001$, 1-way ANOVA followed by Dunnett's multiple comparisons test, $n = 10$ from 3 independent experiments.

conformation transition resolved by PLA changes during maturation of the AIS, we performed gAnkG PLA at 2 critical AIS developmental stages. The first stage was 3 to 4 d in vitro (DIV) of culture when gAnkG was just beginning to be expressed and accumulates in a diffuse pattern along the axon (Fig. 7 *A*, *Left* and *Top* and Fig. 7 *B*, *Left*). Later at 7 DIV, gAnkG accumulation at the AIS was more intense and confined to the proximal axon (Fig. 7 *A*, *Bottom* and Fig. 7 *B*, *Left*). Interestingly, in 4 DIV neurons, β4-spectrin was not detectable at the AIS (Fig. 7 *A*, *Top Middle* and Fig. 7 *B*, *Right*). In contrast, β4-spectrin was highly enriched at the AIS in 7 DIV neurons (Fig. 7 *A*, *Bottom Right* and Fig. 7 *B*, *Right*). To determine if the gAnkG conformation changes during AIS development, we examined endogenous AnkG by PLA as in Fig. 6 in either 4 DIV or 7 DIV neurons. We observed a PLA signal at the AIS in 4 DIV neurons that was largely eliminated in 7 DIV neurons (Fig. 7 *C* and *D*; $P = 0.0002$, *t* test; $n = 10$). Taken together, our results are consistent with the hypothesis that N- and C-terminal domains of gAnkG are in close proximity in immature neurons when the incipient AIS is longer and less concentrated and before β4-spectrin is fully recruited. gAnkG switches to an extended conformation in older neurons, when the AIS becomes shorter with more intense gAnkG labeling, and beta 4-spectrin is highly enriched at the AIS (Fig. 7*E*).

Discussion

We identify a mechanism required for normal neural development in humans that ensures ordered assembly of gAnkG and β4-spectrin at axon initial segments. gAnkG initially targets to the proximal axon configured with close apposition of N- and C-terminal domains revealed by proximity ligation assay. gAnkG in this closed conformation cannot bind to β4-spectrin, but can recruit its membrane-spanning partners 186 kDa neurofascin and voltage-gated sodium channels, although at lower density and in a more elongated pattern than in the mature AIS. Later in development, gAnkG transitions to an extended conformation, resulting in gain of recruitment of β4-spectrin accompanied by maturation of the AIS to a shorter length with higher density of gAnkG and membrane partners. Conversion of gAnkG to an extended conformation capable of binding β4-spectrin is blocked by human neurodevelopmental mutations (T1861M, P2490L, and K2864N) and by mutations preventing phosphorylation (S1982A and S2619A), which are residues all located in the gAnkG neurospecific domain. Together, these findings resolve a discrete intermediate stage in AIS assembly that is regulated through phosphorylation of gAnkG.

Humans bearing compound heterozygous missense mutations (T1861M, P2490L, and K2864N) in the neurospecific domain of gAnkG exhibit multiple disorders, including delayed speech, intellectual impairment, and seizures (*SI Appendix*, Table S1). We found that transfection of ankyrin-G-null neurons with gAnkG bearing these mutations results in a similar cellular phenotype to neurons from *qv3J* mice lacking β4-spectrin (27, 49). In both cases, gAnkG and voltage-gated sodium channels are configured in an elongated and low-density pattern in the proximal axon, and β4-spectrin polypeptides are missing. Neef and colleagues have performed detailed modeling and direct electrophysiological measurements of *qv3J* neurons (50). They concluded that even though sodium channel density is markedly reduced, the elongated axon initial segments of β4-spectrin-deficient neurons still fire action potentials, although with reduced temporal precision. This counterintuitive result derives in part from greater electrical isolation from the neuronal cell body and dendrites due to the elongated axonal geometry, which results both in a lower threshold for action potential initiation as well as a slightly slower responses to dendritic signaling. In addition, β4-spectrin-deficient mice may exhibit homeostatic compensation due to up-regulation of ion channels such as KCNA1 (51). Loss of precise temporal resolution while retaining basic neural signaling is consistent with abnormal acoustic brainstem responses and central deafness noted in *qv* mice that survive to adulthood (51).

Although this study has focused on the AIS, gAnkG mutations may also affect assembly/function of CNS nodes of Ranvier,

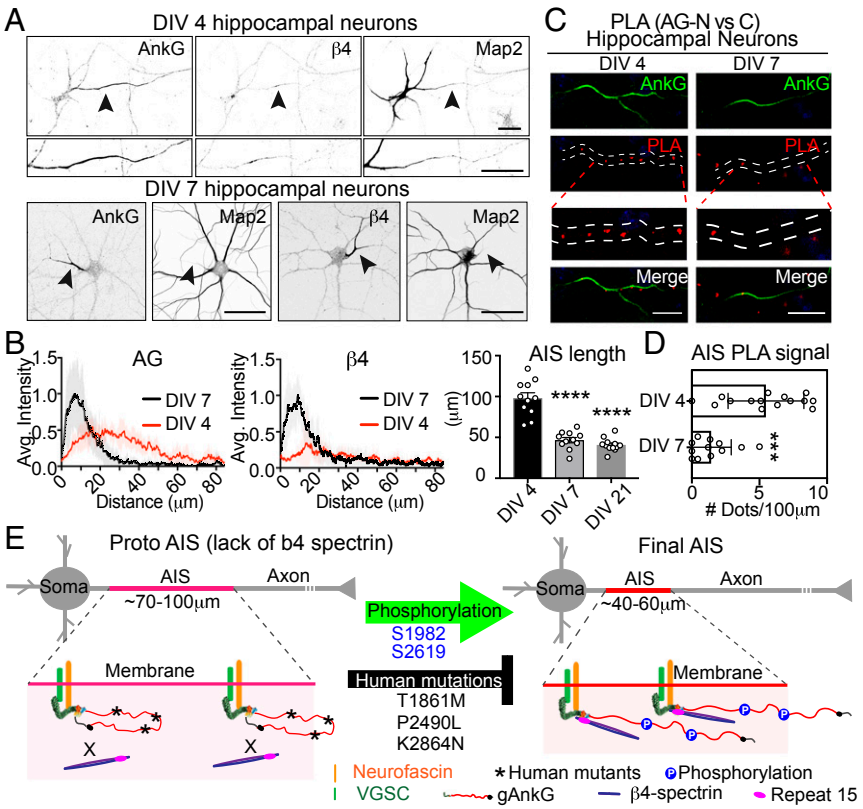

Fig. 7. Gain of an extended conformation of gAnkG and β4-spectrin recruitment to the AIS during neuron development. (*A*) The 4 DIV and 7 DIV hippocampal neurons were stained for AnkG, β4-spectrin, or MAP2. Black arrowheads point to the AIS (Scale bar, 20 μm.) (*B*) Average intensities of AnkG or β4-spectrin at the AIS are plotted for day 4 neurons (red line) and aligned with 7 DIV neurons (black line). The length of AIS is quantified at 3, 7, and 21 DIV. Mean ± SEM, $****P < 0.0001$, 1-way ANOVA followed by Dunnett's multiple comparisons test. $n = 10$ from 3 independent experiments. (*C*) PLA of 4 or 7 DIV neurons using antibodies against N- and C-terminal of AnkG. Representative images of AnkG and PLA at the AIS are shown (Scale bar, 20 μm.) (*D*) PLA signal at the AIS is quantified. Mean ± SEM, $***P = 0.0001$, *t* test. $n = 10$ from 3 independent experiments. (*E*) Schematic showing a proposed conformation change of gAnkG and the recruitment of β4-spectrin in proto-AIS and mature AIS.

which are morphologically abnormal in mice lacking gAnkG (22). In addition, humans bearing gAnkG mutations retain normal 190 kDa ankG, which may compensate at least partially for loss of gAnkG function. For example, mice lacking gAnkG exhibit a 5- to 8-fold increase in 190 kDa ankG, which may contribute to their survival until PND20. These considerations suggest that physiological consequences of gAnkG mutations may be complicated and will be best appreciated using mutant mice.

β4-spectrin has been proposed to coordinate CaMK2 with its voltage-gated sodium channel substrate through binding to AnkG in excitable membranes of heart and the AIS in neurons (17). It is of interest in this regard that the sigma 6 isoform of β4-spectrin, which lacks actin- and adducin-binding domains but retains ability to bind to AnkG and CaMK2, was fully capable of restoring a compact, densely populated AIS in β4-spectin knockout neurons (Fig. 3 *E* and *F*). This finding is consistent with the report by Komada and colleagues that knockout of only sigma 1 β4-spectrin in mice resulted in axon initial segments of normal length, while knockout of both sigma 1 and sigma 6 isoforms resulted in elongated AIS with reduced density of gAnkG and VGSC (49). These considerations suggest that sigma 6 β4-spectrin promotes maturation of the AIS independently from its association with actin, and may act through recruitment of CaMK2 and perhaps other protein kinases. Moreover, if β4-spectrin promotes signaling, modulating phosphorylation at the AIS through activating protein kinase(s) or inhibiting protein phosphatase(s) may offer a therapeutic strategy to treat individuals bearing gAnkG neurodevelopmental mutations.

We observed a strong correlation between an extended conformation of gAnkG and gAnkG activity in binding and AIS recruitment of β4-spectrin. These observations imply that the gAnkG-binding site(s) for beta-4 spectrin is inaccessible in its closed conformation and becomes functional only in the extended conformation. gAnkG may interact with beta-4 spectrin solely through its canonical site located in the ZU5 domain. It also is possible that gAnkG contains a second site specific for beta-4 spectrin that is located in its neurospecific domain and is blocked in the closed conformation. gAnkG has been directly imaged at the AIS in an extended conformation by immunogold label platinum replica electron microscopy (22, 30). However, gAnkG in a closed conformation has been inferred based on proximity ligation signal with antibodies against N- and C-terminal ends, but has not yet been visualized. In addition to imaging gAnkG in its closed conformation, it also will be important in the future to resolve binding interactions between gAnkG and 190 kDa ankG with beta-2 and beta-4 spectrins at an atomic level.

The mechanism underlying preservation of the closed conformation in gAnkG bearing human mutation remains to be determined. One possibility is that mutation at these sites somehow impairs phosphorylation. However, the mutation sites (T1861, P2490, and K2864) are not close to sites of phosphorylation (S1982 and S2619), suggesting that mutation directly affects intramolecular interactions and/or conformation of the neurospecific domain. It is of interest in this regard that the neurospecific domain contains multiple regions predicted to be

intrinsically disordered. Disordered proteins can be in a metastable state capable of gaining long-range folding following phosphorylation or other perturbations (52).

This study identifies a role for gAnkG as a signal integrator at the AIS. We found that the neurospecific domain of gAnkG is phosphorylated at high stoichiometry at multiple residues in adult brain (Fig. 4*A*). In a functional screen of individual major phosphorylated residues, we determined that phosphorylation of S1982 and S2619 is required for gAnkG to associate with β4-spectrin and to recruit β4-spectrin to the AIS as well as for conversion of gAnkG from a closed conformation with close contact between N- and C-terminal domains to an extended conformation. Our screen was based on individual mutations, and would have missed sites that require multiple phosphorylation events. The protein kinase(s) and protein phosphatase(s) that determine the phosphorylation state of gAnkG at axon initial segments remain to be identified. Current candidate protein kinases include protein kinase CK2, which phosphorylates voltage-gated sodium channels and KCNQ2/3 channels, and promotes their binding to gAnkG (12), myosin light chain kinase, which promotes myosin II activity required for AIS assembly (16), and cyclin-dependent protein kinase, which phosphorylates the auxiliary Kvbeta-2 subunit of Kv1 channels and regulates their axonal targeting (53). Grubb and colleagues have identified calcineurin, a calcium- and calmodulin-regulated serine/threonine phosphoprotein phosphatase, as a mediator of activity-dependent structural plasticity of the AIS (15). It is likely that protein kinases/phosphatases act on multiple sites in the same protein substrates as well as multiple proteins to achieve concerted outcomes such as displacement of the entire AIS (8, 9). It also is likely that the repertoire of kinases/phosphatases varies among different types of neurons and also depends on their developmental stage. A challenge for future work will be to elucidate the regulatory networks at the AIS and their function in the context of adaptive neural circuits.

Materials and Methods

Detailed materials and methods can be found in *SI Appendix, SI Materials and Methods*. For the ANK3 mutation study, the family was consented under the protocol of Pro00020102 entitled "Molecular analysis of children with autism spectrum disorder of unknown etiology," approved by Duke Institutional Review Board.

ACKNOWLEDGMENTS. We thank E. Robinson and J. Hostettler for technical assistance, J. Cheong for data analysis, and Dr. Erik Soderblom and Dr. Greg Waitt at Duke University School of Medicine Proteomics and Metabolomics Shared Resource for providing the MS/MS service. This work was supported by the Howard Hughes Medical Institute and a George Barth Geller endowed professorship (V.B.), and National Institutes of Health grants R21MH115155 (V.B.) and F31NS096848 (K.K.W.-C.).

1. M. H. Kole, G. J. Stuart, Signal processing in the axon initial segment. *Neuron* **73**, 235–247 (2012).
2. K. J. Bender, L. O. Trussell, The physiology of the axon initial segment. *Annu. Rev. Neurosci.* **35**, 249–265 (2012).
3. M. N. Rasband, The axon initial segment and the maintenance of neuronal polarity. *Nat. Rev. Neurosci.* **11**, 552–562 (2010).
4. C. Leterrier, The axon initial segment: An updated viewpoint. *J. Neurosci.* **38**, 2135–2145 (2018).
5. J. Szentágothai, M. A. Arbib, Conceptual models of neural organization. *Neurosci. Res. Program Bull.* **12**, 305–510 (1974).
6. P. Somogyi, A specific 'axo-axonal' interneuron in the visual cortex of the rat. *Brain Res.* **136**, 345–350 (1977).
7. T. J. Viney *et al.*, Network state-dependent inhibition of identified hippocampal CA3 axo-axonic cells in vivo. *Nat. Neurosci.* **16**, 1802–1811 (2013).
8. M. S. Grubb, J. Burrone, Activity-dependent relocation of the axon initial segment fine-tunes neuronal excitability. *Nature* **465**, 1070–1074 (2010).
9. H. Kuba, Y. Oichi, H. Ohmori, Presynaptic activity regulates Na(+) channel distribution at the axon initial segment. *Nature* **465**, 1075–1078 (2010).
10. H. Kuba, R. Yamada, G. Ishiguro, R. Adachi, Redistribution of Kv1 and Kv7 enhances neuronal excitability during structural axon initial segment plasticity. *Nat. Commun.* **6**, 8815 (2015).
11. A. Gutzmann *et al.*, A period of structural plasticity at the axon initial segment in developing visual cortex. *Front. Neuroanat.* **8**, 11 (2014).
12. A. Bréchet *et al.*, Protein kinase CK2 contributes to the organization of sodium channels in axonal membranes by regulating their interactions with ankyrin G. *J. Cell Biol.* **183**, 1101–1114 (2008).
13. M. Xu, E. C. Cooper, An ankyrin-G N-terminal gate and protein kinase CK2 dually regulate binding of voltage-gated sodium and KCNQ2/3 potassium channels. *J. Biol. Chem.* **290**, 16619–16632 (2015).
14. J. Lezmy *et al.*, M-current inhibition rapidly induces a unique CK2-dependent plasticity of the axon initial segment. *Proc. Natl. Acad. Sci. U.S.A.* **114**, E10234–E10243 (2017).
15. M. D. Evans, C. Tufo, A. S. Dumitrescu, M. S. Grubb, Myosin II activity is required for structural plasticity at the axon initial segment. *Eur. J. Neurosci.* **46**, 1751–1757 (2017).
16. S. L. Berger *et al.*, Localized myosin II activity regulates assembly and plasticity of the axon initial segment. *Neuron* **97**, 555–570.e6 (2018).
17. T. J. Hund *et al.*, A β(IV)-spectrin/CaMKII signaling complex is essential for membrane excitability in mice. *J. Clin. Invest.* **120**, 3508–3519 (2010).
18. M. D. Evans, A. S. Dumitrescu, D. L. H. Kruijssen, S. E. Taylor, M. S. Grubb, Rapid modulation of axon initial segment length influences repetitive spike firing. *Cell Rep.* **13**, 1233–1245 (2015).
19. V. Bennett, D. N. Lorenzo, An adaptable spectrin/ankyrin-based mechanism for long-range organization of plasma membranes in vertebrate tissues. *Curr. Top. Membr.* **77**, 143–184 (2016).
20. S. M. Jenkins, V. Bennett, Ankyrin-G coordinates assembly of the spectrin-based membrane skeleton, voltage-gated sodium channels, and L1 CAMs at Purkinje neuron initial segments. *J. Cell Biol.* **155**, 739–746 (2001).
21. K. L. Hedstrom, Y. Ogawa, M. N. Rasband, AnkyrinG is required for maintenance of the axon initial segment and neuronal polarity. *J. Cell Biol.* **183**, 635–640 (2008).
22. P. M. Jenkins *et al.*, Giant ankyrin-G: A critical innovation in vertebrate evolution of fast and integrated neuronal signaling. *Proc. Natl. Acad. Sci. U.S.A.* **112**, 957–964 (2015).
23. A. Fréal *et al.*, Cooperative interactions between 480 kDa ankyrin-G and EB proteins assemble the axon initial segment. *J. Neurosci.* **36**, 4421–4433 (2016).
24. Z. Pan *et al.*, A common ankyrin-G-based mechanism retains KCNQ and NaV channels at electrically active domains of the axon. *J. Neurosci.* **26**, 2599–2613 (2006).
25. E. C. Cooper, Made for "anchorin": Kv7.2/7.3 (KCNQ2/KCNQ3) channels and the modulation of neuronal excitability in vertebrate axons. *Semin. Cell Dev. Biol.* **22**, 185–192 (2011).
26. J. Q. Davis, S. Lambert, V. Bennett, Molecular composition of the node of ranvier: Identification of ankyrin-binding cell adhesion molecules neurofascin (mucin+/third FNIII domain-) and NrCAM at nodal axon segments. *J. Cell Biol.* **135**, 1355–1367 (1996).
27. M. Komada, P. Soriano, [Beta]IV-spectrin regulates sodium channel clustering through ankyrin-G at axon initial segments and nodes of Ranvier. *J. Cell Biol.* **156**, 337–348 (2002).
28. Y. Yang, Y. Ogawa, K. L. Hedstrom, M. N. Rasband, betaIV spectrin is recruited to axon initial segments and nodes of Ranvier by ankyrinG. *J. Cell Biol.* **176**, 509–519 (2007).
29. J. M. Sobotzik *et al.*, AnkyrinG is required to maintain axo-dendritic polarity in vivo. *Proc. Natl. Acad. Sci. U.S.A.* **106**, 17564–17569 (2009).
30. S. L. Jones, F. Korobova, T. Svitkina, Axon initial segment cytoskeleton comprises a multiprotein submembranous coat containing sparse actin filaments. *J. Cell Biol.* **205**, 67–81 (2014).
31. E. Kordeli, S. Lambert, V. Bennett, AnkyrinG. A new ankyrin gene with neural-specific isoforms localized at the axonal initial segment and node of Ranvier. *J. Biol. Chem.* **270**, 2352–2359 (1995).
32. V. Bennett, D. N. Lorenzo, Spectrin- and ankyrin-based membrane domains and the evolution of vertebrates. *Curr. Top. Membr.* **72**, 1–37 (2013).
33. V. Bennett, K. Walder, Evolution in action: Giant ankyrins awake. *Dev. Cell* **33**, 1–2 (2015).
34. X. Zhang, V. Bennett, Identification of O-linked N-acetylglucosamine modification of ankyrinG isoforms targeted to nodes of Ranvier. *J. Biol. Chem.* **271**, 31391–31398 (1996).
35. W. C. Tseng, P. M. Jenkins, M. Tanaka, R. Mooney, V. Bennett, Giant ankyrin-G stabilizes somatodendritic GABAergic synapses through opposing endocytosis of GABAA receptors. *Proc. Natl. Acad. Sci. U.S.A.* **112**, 1214–1219 (2015).
36. J. Li *et al.*, Potent and specific Atg8-targeting autophagy inhibitory peptides from giant ankyrins. *Nat. Chem. Biol.* **14**, 778–787 (2018).
37. M. Kuijpers *et al.*, Dynein regulator NDEL1 controls polarized cargo transport at the axon initial segment. *Neuron* **89**, 461–471 (2016).
38. A. D. Nelson *et al.*, Ankyrin-G regulates forebrain connectivity and network synchronization via interaction with GABARAP. *Mol. Psychiatry* 10.1038/s41380-018-0308-x (2018).
39. Z. Iqbal *et al.*, Homozygous and heterozygous disruptions of ANK3: At the crossroads of neurodevelopmental and psychiatric disorders. *Hum. Mol. Genet.* **22**, 1960–1970 (2013).
40. S. Lacas-Gervais *et al.*, BetaIVSigma1 spectrin stabilizes the nodes of Ranvier and axon initial segments. *J. Cell Biol.* **166**, 983–990 (2004).
41. Y. Srinivasan, L. Elmer, J. Davis, V. Bennett, K. Angelides, Ankyrin and spectrin associate with voltage-dependent sodium channels in brain. *Nature* **333**, 177–180 (1988).
42. J. J. Ipsaro, A. Mondragón, Structural basis for spectrin recognition by ankyrin. *Blood* **115**, 4093–4101 (2010).
43. M. He, K. M. Abdi, V. Bennett, Ankyrin-G palmitoylation and βII-spectrin binding to phosphoinositide lipids drive lateral membrane assembly. *J. Cell Biol.* **206**, 273–288 (2014).

44. X. Zhang, V. Bennett, Restriction of 480/270-kD ankyrin G to axon proximal segments requires multiple ankyrin G-specific domains. *J. Cell Biol.* **142**, 1571–1581 (1998).
45. K. Chen, J. Li, C. Wang, Z. Wei, M. Zhang, Autoinhibition of ankyrin-B/G membrane target bindings by intrinsically disordered segments from the tail regions. *eLife* **6**, e29150 (2017).
46. K. Kizhatil *et al*., Ankyrin-G and beta2-spectrin collaborate in biogenesis of lateral membrane of human bronchial epithelial cells. *J. Biol. Chem.* **282**, 2029–2037 (2007).
47. M. He, W. C. Tseng, V. Bennett, A single divergent exon inhibits ankyrin-B association with the plasma membrane. *J. Biol. Chem.* **288**, 14769–14779 (2013).
48. A. Schlüter *et al*., Structural plasticity of synaptopodin in the axon initial segment during visual cortex development. *Cereb. Cortex* **27**, 4662–4675 (2017).
49. Y. Uemoto *et al*., Specific role of the truncated betaIV-spectrin Sigma6 in sodium channel clustering at axon initial segments and nodes of ranvier. *J. Biol. Chem.* **282**, 6548–6555 (2007).
50. E. Lazarov *et al*., An axon initial segment is required for temporal precision in action potential encoding by neuronal populations. *Sci. Adv.* **4**, eaau8621 (2018).
51. N. J. Parkinson *et al*., Mutant beta-spectrin 4 causes auditory and motor neuropathies in quivering mice. *Nat. Genet.* **29**, 61–65 (2001).
52. P. Kulkarni *et al*., Structural metamorphism and polymorphism in proteins on the brink of thermodynamic stability. *Protein Sci.* **27**, 1557–1567 (2018).
53. H. Vacher *et al*., Cdk-mediated phosphorylation of the Kvβ2 auxiliary subunit regulates Kv1 channel axonal targeting. *J. Cell Biol.* **192**, 813–824 (2011).